Microstructural and optical properties of CdSe/CdS/ZnS core-shell-shell quantum dots

Dea Uk Lee,[1] Dae Hun Kim,[1] Dong Hyuk Choi,[2] Sang Wook Kim,[2] Hong Seok Lee,[3] Keon-Ho Yoo,[4] and Tae Whan Kim[1,*]

[1]*Department of Electronics and Computer Engineering, Hanyang University, Seoul 04763, South Korea*
[2]*Department of Molecular Science & Technology, Ajou University, Suwon 16449, South Korea*
[3]*Department of Physics, Research Institute of Physics and Chemistry, Chonbuk National University, Jeonju 54896, South Korea*
[4] *Department of Physics and Research Institute for Basic Sciences, Kyung Hee University, Seoul 02447, South Korea*
[*]*twk@hanyang.ac.kr*

Abstract: CdSe/CdS/ZnS core-shell-shell quantum dots (QDs) were synthesized by using a solution process. High-resolution transmission electron microscopy images and energy dispersive spectroscopy profiles confirmed that stoichiometric CdSe/CdS/ZnS core-shell-shell QDs were formed. Ultraviolet-visible absorption and photoluminescence (PL) spectra of CdSe/CdS/ZnS core-shell-shell QDs showed the dominant excitonic transitions from the ground electronic subband to the ground hole subband ($1S(e)$-$1S_{3/2}(h)$). The PL mechanism is suggested; the carriers generated by the exciting high-energy photons in the shell region are relaxed to the band-edge states of the core region and recombined to emit lower-energy photons. The activation energy of the carriers confined in the CdSe/CdS/ZnS core-shell-shell QDs, as obtained from temperature-dependent PL spectra, was 200 meV. The quantum efficiency of the CdSe/CdS/ZnS core-shell-shell QDs at 300 K was estimated to be approximately 57%.

OCIS codes: (270.5580) Quantum electrodynamics; (160.6000) Semiconductor materials; (020.5580) Quantum electrodynamics.

References and links

1. F. Wang, R. Deng, J. Wang, Q. Wang, Y. Han, H. Zhu, X. Chen, and X. Liu, "Tuning upconversion through energy migration in core-shell nanoparticles," Nat. Mater. **10**(12), 968–973 (2011).
2. K. W. Han, M. H. Lee, D. Y. Yun, T. W. Kim, S. W. Kim, and S.-W. Kim, "Electrical characteristics and operating mechanisms of nonvolatile memory devices fabricated utilizing core-shell $CuInS_2$-ZnS quantum dots embedded in a poly(methyl methacrylate) layer," Appl. Phys. Lett. **99**(19), 193302 (2011).
3. D. Y. Yun, W. S. Song, T. W. Kim, S. W. Kim, and S. W. Kim, "Electrical stabilities and carrier transport mechanisms of flexible organic bistable devices fabricated utilizing CdSe-InP core-shell nanoparticles/polystyrene nanocomposites," Appl. Phys. Lett. **101**(10), 103305 (2012).
4. L. Etgar, D. Yanover, R. K. Capek, R. Vaxenburg, Z. Xue, B. Liu, M. K. Nazeeruddin, E. Lifshitz, and M. Grätzel, "Core/shell PbSe/PbS QDs TiO_2 heterojunction solar cell," Adv. Funct. Mater. **23**(21), 2736–2741 (2013).
5. O. Chen, J. Zhao, V. P. Chauhan, J. Cui, C. Wong, D. K. Harris, H. Wei, H.-S. Han, D. Fukumura, R. K. Jain, and M. G. Bawendi, "Compact high-quality CdSe-CdS core-shell nanocrystals with narrow emission linewidths and suppressed blinking," Nat. Mater. **12**(5), 445–451 (2013).
6. Y. Yang, Z. Liu, and T. Lian, "Bulk transport and interfacial transfer dynamics of photogenerated carriers in CdSe quantum dot solid electrodes," Nano Lett. **13**(8), 3678–3683 (2013).
7. W. Ji, P. Jing, W. Xu, X. Yuan, Y. Wang, J. Zhao, and A. K.-Y. Jen, "High color purity ZnSe/ZnS core/shell quantum dot based blue light emitting diodes with an inverted device structure," Appl. Phys. Lett. **103**(5), 053106 (2013).
8. W. Chen, F. Li, C. Wu, and T. Guo, "Optical properties of fluorescent zigzag graphene quantum dots derived from multi-walled carbon nanotubes," Appl. Phys. Lett. **104**(6), 063109 (2014).
9. B. O. Dabbousi, J. Rodriguez-Viejo, F. V. Mikulec, J. R. Heine, H. Mattoussi, R. Ober, K. F. Jensen, and M. G. Bawendi, "(CdSe)ZnS core-shell quantum dots: Synthesis and characterization of a size series of highly luminescent nanocrystallites," J. Phys. Chem. B **101**(46), 9463–9475 (1997).

#253011 Received 30 Oct 2015; revised 9 Dec 2015; accepted 18 Dec 2015; published 22 Dec 2015

10. D. V. Talapin, A. L. Rogach, A. Kornowski, M. Haase, and H. Weller, "Highly luminescent monodisperse CdSe and CdSe/ZnS nanocrystals synthesized in a hexadecylamine-trioctylphosphine oxide-trioctylphospine mixture," Nano Lett. **1**(4), 207–211 (2001).
11. M. Anni, L. Manna, R. Cingolani, D. Valerini, A. Cretí, and M. Lomascolo, "Förster energy transfer from blue-emitting polymers to colloidal CdSe/ZnS core shell quantum dots," Appl. Phys. Lett. **85**(18), 4169–4171 (2004).
12. R. Wargnier, A. V. Baranov, V. G. Maslov, V. Stsiapura, M. Artemyev, M. Pluot, A. Sukhanova, and I. Nabiev, "Energy transfer in aqueous solutions of oppositely charged CdSe/ZnS core/shell quantum dots and in quantum dot-nanogold assemblies," Nano Lett. **4**(3), 451–457 (2004).
13. S. Nizamoglu, T. Ozel, E. Sari, and H. V. Demir, "White light generation using CdSe/ZnS core–shell nanocrystals hybridized with InGaN/GaN light emitting diodes," Nanotechnology **18**(6), 065709 (2007).
14. F. Li, D. I. Son, J. H. Ham, B. J. Kim, J. H. Jung, and T. W. Kim, "Memory effect of nonvolatile bistable devices based on CdSe/ZnS nanoparticles sandwiched between C_{60} layers," Appl. Phys. Lett. **91**(16), 162109 (2007).
15. M. A. Osborne and S. F. Lee, "Quantum dot photoluminescence activation and decay: dark, bright, and reversible populations in ZnS-capped CdSe nanocrystals," ACS Nano **5**(10), 8295–8304 (2011).
16. W. J. Kwon, S. H. Kim, K. S. Lee, D. C. Choo, S. W. Kim, S.-W. Kim, T. W. Yoo, M. S. Kwon, K. H. Yoo, and T. W. Kim, "Color stability of white organic light emitting devices with a color conversion layer utilizing CdSe/ZnS quantum dots and phosphors dispersed in polymethylmethacrylate," J. Nanosci. Nanotechnol. **13**(6), 4390–4393 (2013).
17. D. V. Talapin, I. Mekis, S. Götzinger, A. Kornowski, O. Benson, and H. Weller, "CdSe/CdS/ZnS and CdSe/ZnSe/ZnS core-shell-shell nanocrystals," J. Phys. Chem. B **108**(49), 18826–18831 (2004).
18. Z. Ma, P. C. Ooi, F. Li, D. Y. Yun, and T. W. Kim, "Electrical bistabilities and conduction mechanisms of nonvolatile memories based on a polymethylsilsesquioxane insulating layer containing CdSe/ZnS quantum dots," J. Electron. Mater. **44**(10), 3962–3966 (2015).
19. K. H. Kim, S. J. Park, Y. P. Jeon, and T. W. Kim, "Luminance enhancement of color stabilized organic light-emitting devices with an active layer containing CdSe/CdS/ZnS core/shell/shell quantum dots," J. Nanosci. Nanotechnol. **14**(11), 8352–8355 (2014).
20. J. Lim, S. Jun, E. Jang, H. Baik, H. Kim, and J. Cho, "Preparation of highly luminescent nanocrystals and their application to light-emitting diodes," Adv. Mater. **19**(15), 1927–1932 (2007).
21. S. Rosen, O. Schwartz, and D. Oron, "Transient fluorescence of the off state in blinking CdSe/CdS/ZnS semiconductor nanocrystals is not governed by Auger recombination," Phys. Rev. Lett. **104**(15), 157404 (2010).
22. X. Wang, W. Li, and K. Sun, "Stable efficient CdSe/CdS/ZnS core/multi-shell nanophosphors fabricated through a phosphine-free route for white light-emitting-diodes with high color rendering properties," J. Mater. Chem. **21**(24), 8558–8565 (2011).
23. Y. Wang, V. D. Ta, Y. Gao, T. C. He, R. Chen, E. Mutlugun, H. V. Demir, and H. D. Sun, "Stimulated emission and lasing from CdSe/CdS/ZnS core-multi-shell quantum dots by simultaneous three-photon absorption," Adv. Mater. **26**(18), 2954–2961 (2014).
24. V. I. Klimov, "Spectral and dynamical properties of multiexcitons in semiconductor nanocrystals," Annu. Rev. Phys. Chem. **58**(1), 635–673 (2007).
25. O. Chen, J. Zhao, V. P. Chauhan, J. Cui, C. Wong, D. K. Harris, H. Wei, H.-S. Han, D. Fukumura, R. K. Jain, and M. G. Bawendi, "Compact high-quality CdSe-CdS core-shell nanocrystals with narrow emission linewidths and suppressed blinking," Nat. Mater. **12**(5), 445–451 (2013).
26. F. Purcell-Milton and Y. K. Gun'ko, "Quantum dots for luminescent solar concentrators," J. Mater. Chem. **22**(33), 16687–16697 (2012).
27. I. Coropceanu and M. G. Bawendi, "Core/shell quantum dot based luminescent solar concentrators with reduced reabsorption and enhanced efficiency," Nano Lett. **14**(7), 4097–4101 (2014).
28. Y. Choi, C. Yim, S. Baek, M. Choi, S. Jeon, and K. Yong, "In situ measurement of photostability of CdSe/CdS/ZnO nanowires photoelectrode for photoelectrochemical water splitting," Sens. Actuators B Chem. **221**, 113–119 (2015).
29. Y. Terai, S. Kuroda, K. Takita, T. Okuno, and Y. Masumoto, "Zero-dimensional excitonic properties of self-organized quantum dots of CdTe grown by molecular beam epitaxy," Appl. Phys. Lett. **73**(25), 3757–3759 (1998).
30. X. D. Mu, Y. J. Ding, B. S. Ooi, and M. Hopkinson, "Investigation of carrier dynamics on InAs quantum dots embedded in InGaAs/GaAs quantum wells based on time-resolved pump and probe differential photoluminescence," Appl. Phys. Lett. **89**(18), 181924 (2006).
31. E. M. Daly, T. J. Glynn, J. D. Lambkin, L. Considine, and S. Walsh, "Behavior of $In_{0.48}Ga_{0.52}P/(Al_{0.2}Ga_{0.8})_{0.52}In_{0.48}P$ quantum-well luminescence as a function of temperature," Phys. Rev. B Condens. Matter **52**(7), 4696–4699 (1995).
32. E. Y. Lin, C. Y. Chen, T. S. Lay, T. C. Wang, J. D. Tsay, P. X. Peng, and T. Y. Lin, "Internal quantum efficiency and optical polarization analysis of InGaN/GaN multiple quantum wells on a-plane GaN," Phys. Status Solidi, C Conf. Crit. Rev. **5**(6), 2111–2113 (2008).
33. S. Watanabe, N. Yamada, M. Nagashima, Y. Ueki, C. Sasaki, Y. Yamada, T. Taguchi, K. Tadatomo, H. Okagawa, and H. Kudo, "Internal quantum efficiency of highly-efficient InxGa1-xN-based near-ultraviolet light-emitting diodes," Appl. Phys. Lett. **83**(24), 4906–4908 (2003).

#253011 Received 30 Oct 2015; revised 9 Dec 2015; accepted 18 Dec 2015; published 22 Dec 2015

1. Introduction

Semiconductor core-shell quantum dots (QDs) have been particularly attractive because of interest in investigations of fundamental physics and their promising potential applications for electronic and optoelectronic devices, such as memory devices, light-emitting devices, and solar cells [1–5]. The prospect of potential applications of core-shell QDs has driven extensive efforts to control precisely the core sizes and the shell thicknesses of the QDs because their optical and electronic properties significantly depend on these parameters [6–8]. Among various kinds of core-shell QDs, CdSe/ZnS core-shell QDs [9–16] are one of the most intensively studied kinds; the CdSe core can cover the most of the visible spectrum depending on its size and the ZnS shell with its large bandgap can confine the carriers well. However, CdSe/ZnS core-shell QDs suffer from the defects due to a large lattice mismatch between CdSe and ZnS, and CdS middle shell with intermediate lattice constant was introduced to form CdSe/CdS/ZnS core- shell-shell QDs [17]. The stable organic bistable memory devices were fabricated utilizing CdSe/ZnS core-shell QDs [18], and the luminance efficiency of the organic light-emitting devices was enhanced due to the insertion of the active layer containing CdSe/CdS/ZnS core-shell-shell QDs [19]. Even though some studies concerning the formation and the basic physical properties of the CdSe/CdS/ZnS core-shell-shell QDs have been conducted [19–23], investigations on their interband transitions and activation energy have not been reported yet. Furthermore, studies on the interband transitions and activation energy of CdSe/CdS/ZnS core-shell-shell QDs are very important for improving the efficiencies of electronic and optoelectronic devices based on core-shell-shell QDs.

This paper presents data for the microstructural and optical properties of CdSe/CdS/ZnS core-shell-shell QDs. Transmission electron microscopy (TEM) and energy dispersive X-ray spectroscopy (EDS) measurements were performed to characterize the microstructural and the stoichiometric properties of the CdSe/CdS/ZnS core-shell-shell QDs. Absorption and temperature-dependent photoluminescence (PL) measurements were carried out in order to investigate the interband transitions and to determine the activation energy and the quantum efficiency in the CdSe/CdS/ZnS core-shell-shell QDs.

TEM measurements were performed using JEOL 2010EX and Philips Tecnai F20 with acceleration voltage of 200 kV. The samples for the cross-sectional TEM measurements were prepared by cutting and polishing with sandpaper to a thickness of approximately 10 μm, and were then argon-ion milled to electron transparency. The absorption spectra were measured by using a VARIAN Cary 100 Conc UV/vis spectrophotometer. The PL measurements were carried out using a 50-cm monochromator equipped with an RCA 31034 photomultiplier tube. The excitation source was the 4416-Å line of a He-Cd laser, and the laser power density was 10 mW/cm^2. The sample temperature was controlled between 10 and 350 K by using a He displex system.

2. Experimental details

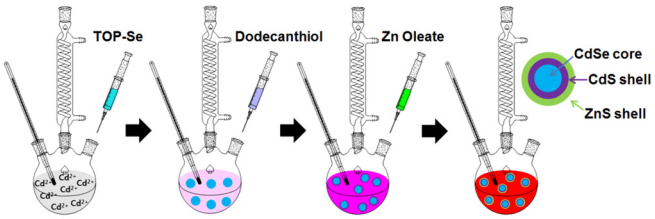

Fig. 1. Schematic illustration of fabrication steps for the CdSe/CdS/ZnS core-shell-shell quantum dots.

The synthesis procedure of CdSe/CdS/ZnS core-shell-shell QDs was described elsewhere [20]. The series of the reaction steps for the synthesis of CdSe/CdS/ZnS core-shell-shell QDs are schematically shown in Fig. 1, and described in detail in the followings. 0.103 g of CdO,

#253011 Received 30 Oct 2015; revised 9 Dec 2015; accepted 18 Dec 2015; published 22 Dec 2015

0.901 g of oleic acid and 20 ml of tri-n-octylamine were loaded into a three-necked flask. The mixture was degassed under vacuum to remove the oxygen and water at 150°C for 1 h. The flask was heated to 300°C by using a heating mantle under N_2 atmosphere, and then the 0.2 ml of TOP-Se solution (1M, Tri-n-octylphosphine base) was injected into the flask at 300°C. The mixture was stirred for 90 sec, and then 0.1 ml of 1-dodecanethiol and 3 ml of tri-n-octylamine were added slowly into the flask at rate of 0.5 ml/min and held at 300°C for 40 min. To form the ZnS shell, 8 ml of Zn Oleate solution was added over 8 minutes in the flask containing CdSe/CdS core-shell QDs at 100°C, and then 0.56 ml of 1-dodecanethiol and 3 ml of tri-n-octylamine were added slowly to the flask at rate of 0.5 ml/min and held at 100°C for 30 min. The solution was workup by using ethanol to produce CdSe/CdS/ZnS core-shell-shell QDs.

3. Results and discussion

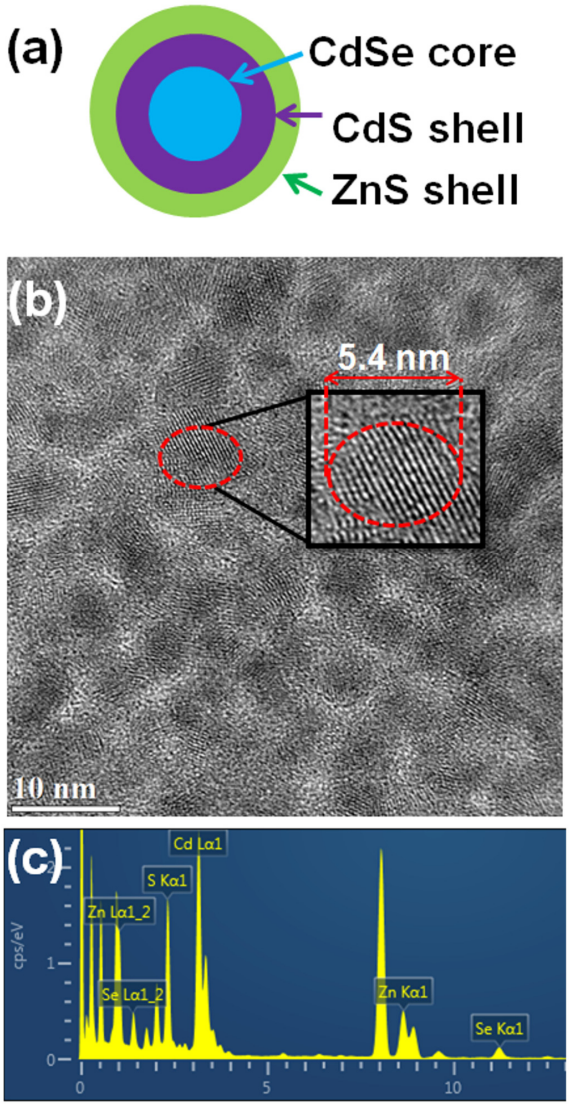

Fig. 2. (a) Schematic diagram of the CdSe/CdS/ZnS core-shell-shell quantum dots. (b) Transmission electron microscopy image, and (c) energy dispersive spectroscopy profile of the CdSe/CdS/ZnS core-shell-shell quantum dots.

#253011 Received 30 Oct 2015; revised 9 Dec 2015; accepted 18 Dec 2015; published 22 Dec 2015

A schematic diagram of CdSe/CdS/ZnS core-shell-shell QDs is shown in Fig. 2(a). Figure 2(b) shows a high-resolution TEM (HRTEM) image of the CdSe/CdS/ZnS core-shell-shell QDs. The HRTEM image reveals the formation of the CdSe/CdS/ZnS core-shell-shell QDs. The typical diameters of the CdSe/CdS/ZnS core-shell-shell QDs are about 5.4 nm. An EDS spectrum with Cd, Se, S, and Zn peaks indicates that the stoichiometric CdSe/CdS/ZnS core-shell-shell QDs are formed, as shown in Fig. 2(c).

Figure 3 shows the linear UV-visible absorption spectrum of CdSe/CdS/ZnS core-shell-shell QDs dispersed in toluene at room temperature. The dominant excitonic transitions from the ground electronic subband to the ground hole subband ($1S(e)$-$1S_{3/2}(h)$) are clearly observed [23, 24]. Two shoulders, one at 538 nm and the other at 498 nm correspond ($1S(e)$-$2S_{3/2}(h)$) and ($1P(e)$-$1P_{3/2}(h)$), respectively [23, 24]. Three clearly resolved lowest excitonic transitions in the absorption spectrum, together with a narrow emission linewidth of the PL spectrum, indicate the high quality of the CdSe/CdS/ZnS core-shell-shell QDs [25].

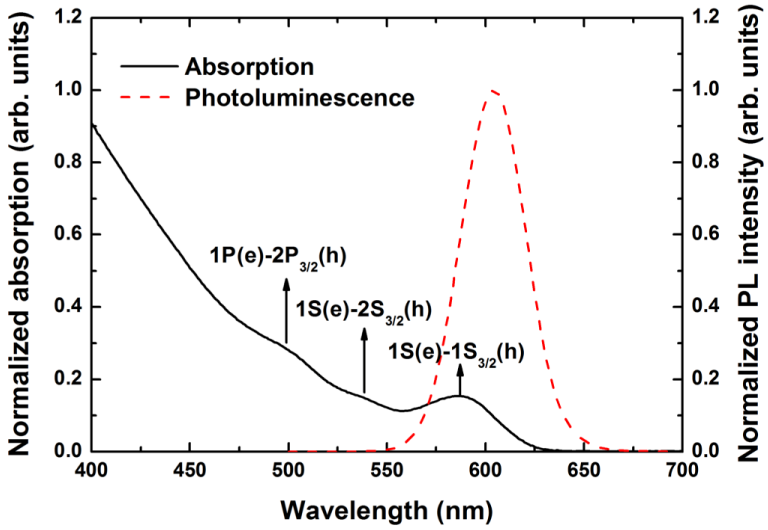

Fig. 3. Normalized UV-visible absorption (solid line) and photoluminescence (dashed line) spectra of the CdSe/CdS/ZnS core-shell-shell quantum dots.

When the UV light with a wavelength of 365 nm is exposed to the CdSe/CdS/ZnS core-shell-shell QDs dispersed in toluene, after the CdSe/CdS/ZnS core-shell-shell QDs absorb the UV lights, the photons with a wavelength of 604 nm are emitted, as shown in Figs. 4(a) and 4(b). The schematic diagram of the optical processes in the CdSe/CdS/ZnS core-shell-shell QDs is shown in Fig. 4(c). The CdSe/CdS/ZnS core-shell-shell QDs allow for a spectral separation of the absorption and emission by confining the two processes to different regions [26]. The fundamental operation process begins with an absorption of the incident photon, in which high photon energies might create electron-hole pairs in the states predominantly located in the shells [27]. Then, electrons and holes are relaxed rapidly to the band-edge states, which are confined within the CdSe core. Finally the exciton recombines radiatively, resulting in the emission of the photons with a different wavelength in comparison with that with incident photons [27]. This carrier movement is in contrast with the case of CdSe/CdS/ZnO nanowires in which electrons move to the ZnO shell and holes move the CdSe core [28].

#253011 Received 30 Oct 2015; revised 9 Dec 2015; accepted 18 Dec 2015; published 22 Dec 2015

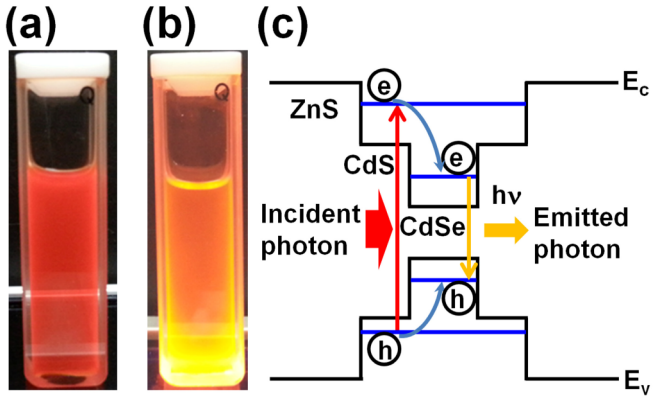

Fig. 4. Images of (a) before and (b) after exposures of UV excitation wavelength of 365 nm for CdSe/CdS/ZnS core-shell-shell quantum dots. (c) Schematic diagram of the optical processes in the CdSe/CdS/ZnS core-shell-shell quantum dots.

Figure 5 shows a PL spectrum for the CdSe/CdS/ZnS core-shell-shell QDs at several temperatures. The dominant peak corresponds to the (1S(e)-1$S_{3/2}$(h)). The peak energy is 2.056 eV at 10 K, and shifts to lower energy with increasing temperature, reaching about 1.968 eV at 300 K. The PL integrated intensity tends to decrease as the temperature increases. The PL quenching at higher temperatures is caused by an escape of carriers via a non-radiative recombination path [29]. However, the integrated PL intensity significantly increases with increasing temperature from 100 to 200 K. This behavior is attributed to the presence of the barriers induced by the strain fields at the interfaces formed between the CdSe/CdS/ZnS core-shell-shell QDs [30].

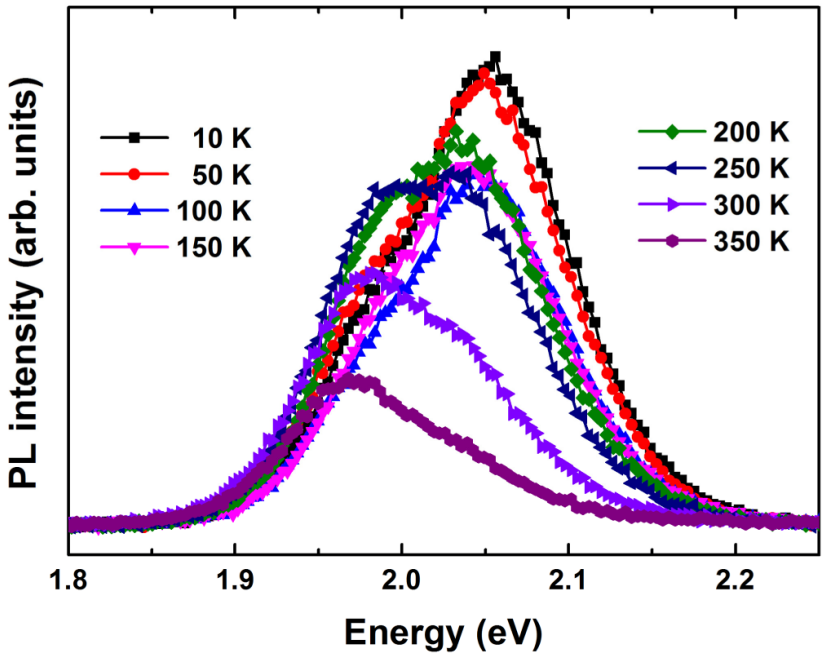

Fig. 5. Photoluminescence spectra measured at several temperatures for CdSe/CdS/ZnS core-shell-shell quantum dots.

As shown in Fig. 6(a), the temperature dependence of the intensity can be fitted using the equation $I = I_0 / \{1 + C[\exp(-E_A/k_BT)]\}$ [31], where I_0 and C are constants and E_A is an

#253011 Received 30 Oct 2015; revised 9 Dec 2015; accepted 18 Dec 2015; published 22 Dec 2015

activation energy that corresponds to the barrier height for the non-radiative recombination path. The activation energy of the carriers confined in the CdSe/CdS/ZnS core-shell-shell QDs, determined by fitting integrated PL intensities as a function of the reciprocal temperature [31], is 200 meV. From the temperature-dependent PL spectra, the quantum efficiency (QE) for the CdSe/CdS/ZnS core-shell-shell QDs at 300 K is analyzed by using the equation of QE(300 K) ≈QE(0 K) × [I(300 K)/I(10 K)] [32]. Because the non-radiative recombination processes for the CdSe/CdS/ZnS core-shell-shell QD is negligible at low temperatures, the QE at 10 K approaches 100% [33]. The ratio [I(300 K)/I(10 K)] was estimated from the integrated PL intensities. These results demonstrate that the QE for the CdSe/CdS/ZnS core-shell-shell QDs at 300 K is estimated to be about 57%, as shown in Fig. 6(b).

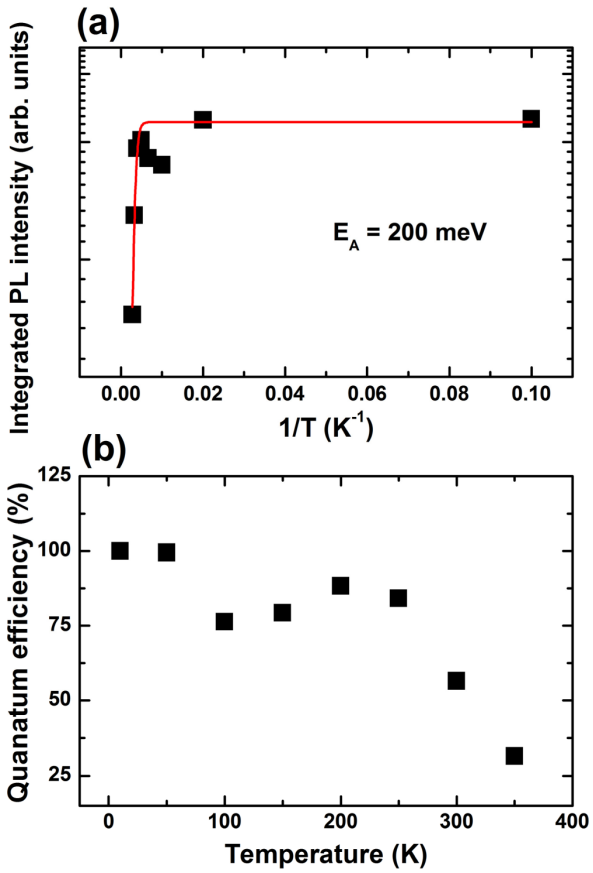

Fig. 6. (a) Integrated photoluminescence intensity as functions of the reciprocal temperature for CdSe/CdS/ZnS core-shell-shell quantum dots. Solid rectangles represent experimental data and the solid line indicates the fitting curve. (b) Quantum efficiency as functions of the temperature for CdSe/CdS/ZnS core-shell-shell quantum dots.

4. Summary and conclusions

CdSe/CdS/ZnS core-shell-shell QDs were synthesized and their microstructural and optical properties were studied. HRTEM images and EDS profiles showed the formation of the stoichiometric CdSe/CdS/ZnS core-shell-shell QDs. Ultraviolet-visible absorption and PL spectra of CdSe/CdS/ZnS core-shell-shell QDs showed the (1S(e)-$1S_{3/2}$(h)) dominant excitonic transitions together with (1S(e)-$2S_{3/2}$(h)) and (1P(e)-$1P_{3/2}$(h)) excitonic transitions. The temperature-dependent PL spectra showed that the peaks corresponding to the (1S(e)-

#253011 Received 30 Oct 2015; revised 9 Dec 2015; accepted 18 Dec 2015; published 22 Dec 2015

$1S_{3/2}$(h)) of the CdSe/CdS/ZnS core-shell-shell QDs shifted to a lower energy side with increasing temperature, the amount of shift being 88 meV between 10 and 300 K. The activation energy of the CdSe/CdS/ZnS core-shell-shell QDs, as determined from the temperature-dependent PL spectra was 200 meV. The QE of the CdSe/CdS/ZnS core-shell-shell QDs at 300 K was approximately 57%. The present results help in improving the understanding of the microstructural and optical properties of CdSe/CdS/ZnS core-shell-shell QDs.

Acknowledgments

This research was supported by Basic Science Research Program through the National Research Foundation of Korea (NRF) funded by the Ministry of Education, Science and Technology (2013R1A2A1A01016467).

#253011 Received 30 Oct 2015; revised 9 Dec 2015; accepted 18 Dec 2015; published 22 Dec 2015